Osmotic Stress and the Yeast Cytoskeleton: Phenotype-specific Suppression of an Actin Mutation

Sumita Chowdhury, Karrie W. Smith, and Michael C. Gustin

Department of Biochemistry and Cell Biology, Wiess School of Natural Sciences, Rice University, P. O. Box 1892, Houston, Texas 77251

Abstract. In the yeast *Saccharomyces cerevisiae*, actin filaments function to direct cell growth to the emerging bud. Yeast has a single essential actin gene, *ACT1*. Diploid cells containing a single copy of *ACT1* are osmosensitive (Osm^S), i.e., they fail to grow in high osmolarity media (D. Shortle, unpublished observations cited by Novick, P., and D. Botstein. 1985. *Cell.* 40:415–426). This phenotype suggests that an underlying physiological process involving actin is osmosensitive. Here, we demonstrate that this physiological process is a rapid and reversible change in actin filament organization in cells exposed to osmotic stress. Filamentous actin was stained using rhodamine phalloidin. Increasing external osmolarity caused a rapid loss of actin filament cables, followed by a slower redistribution of cortical actin filament patches. In the recovery phase, cables and patches were restored to their original levels and locations. Strains containing an *act1-1* mutation are both Osm^S and temperature-sensitive (Ts) (Novick and Botstein, 1985). To identify genes whose products functionally interact with actin in cellular responses to osmotic stress, we have isolated extragenic suppressors which revert only the Osm^S but not the Ts phenotype of an *act1-1* mutant. These suppressors identify three genes, *RAH1–RAH3*. Morphological and genetic properties of a dominant suppressor mutation suggest that the product of the wild-type allele, $RAH3^+$, is an actin-binding protein that interacts with actin to allow reassembly of the cytoskeleton following osmotic stress.

GROWTH in the budding yeast *Saccharomyces cerevisiae* is asymmetrical and directed towards the emerging bud. Morphological and genetic evidence suggests an important role for actin in this process (for a review see Barnes et al., 1990). Using fluorescence microscopy to localize actin filaments in growing yeast cells, Adams and Pringle (1984) and Kilmartin and Adams (1984) observed two types of actin filament-containing structures: long cables and small cortical patches. Cables of actin filaments are found principally in the mother cell, extending along the axis of growth toward the emerging daughter cell. In unbudded cells, cortical patches of actin filaments form a ring surrounding the site of bud emergence. Later, these cortical patches concentrate in the growing bud. As the bud fully enlarges, the patches delocalize throughout the cortex of both mother and daughter cell and then reconcentrate in the neck between the separating cells. The regions where cortical actin filament patches concentrate are also those where active cell wall deposition and cell growth occur (Pringle and Hartwell, 1981), suggesting a causal connection between these phenomena. Phenotypic analysis of yeast actin mutants also gives strong support for the prominent role of actin in yeast morphogenesis. *S. cerevisiae* has a single essential gene for actin, *ACT1* (Gallwitz and Seidel, 1980; Gallwitz and Sures, 1980; Ng and Abelson, 1980; Shortle et al., 1982). Cells carrying temperature-sensitive (Ts)[1] *act1-1* or *act1-2* mutations (Shortle et al., 1984) when grown at the non-permissive temperature have a highly aberrant actin filament distribution. Such cells deposit chitin uniformly over the cell surface instead of at the bud neck, accumulate secretory vesicles, and become enlarged (Novick and Botstein, 1985). These mutant phenotypes are those expected for a defect in proper spatial organization of cell growth.

Yeast can adapt and grow under a variety of environmental conditions. The existence of mechanosensitive ion channels in the yeast plasma membrane (Gustin et al., 1988) suggests that yeast may sense and respond to physical forces such as pressure in their environment. Based on studies in other fungi and in plants (Cosgrove, 1986; Ortega et al., 1989), turgor pressure resulting from the osmotic gradient across the cell membrane is important for cell growth. Cells must respond to an increase in external osmolarity and the subsequent loss of turgor pressure to continue growth. A poorly understood aspect of yeast actin function is its role in the cellular response to osmotic stress. Analysis of actin mutants suggests that normal actin function is required for yeast cells

1. *Abbreviations used in this paper*: Osm^R, osmoresistant; Osm^S, osmosensitive; Rh-phalloidin, rhodamine phalloidin; Ts, temperature sensitive; Ts^L, temperature sensitive lethal.

to grow in high osmolarity media. Novick and Botstein (1985) observed that the Ts *actl-1* or *actl-2* mutants grown at the permissive growth temperature were osmosensitive (Osm^S), failing to grow in high osmolarity media. Diploid cells containing one wild-type copy of actin and one null allele are Osm^S (refer to D. Shortle communication cited in Novick and Botstein, 1985). This result argues that the Osm^S phenotype is not the consequence of a mutant gene product whose stability is osmosensitive but is the result of an osmosensitive physiological process dependent on actin concentration. Here, we demonstrate that this physiological process is a rapid and reversible change in actin filament organization in wild-type cells exposed to osmotic stress.

The mechanism responsible for the changes in actin filament organization in response to osmotic stress is unknown, but presumably reflects changes in the association of actin with other cellular proteins. Many different actin-binding proteins have been identified in eukaryotic cells (Drubin, 1990; Hartwig and Kwiatkowski, 1991; Matsudaira, 1991; Luna, 1991). Although in vitro studies have assigned functions to these proteins, e.g., actin filament capping, severing, and bundling, the in vivo function of many such proteins, particularly their role in specific cellular responses, remains to be determined. The technique of genetic suppressor analysis, applied to the study of the cytoskeleton in yeast (Huffaker et al., 1987), has been used to reveal physiologically relevant interactions between actin and the many proteins that regulate its function in cells (Novick et al., 1989; Adams and Botstein, 1989). The reasoning behind this approach is that actin mutants with a cell growth defect can be suppressed by mutations in proteins which functionally interact with actin. Suppressors of a Ts *actl-1* mutant, isolated by Novick et al. (1989) and Adams and Botstein (1989), have been used to identify six genes, *SAC1–SAC6*, that potentially encode actin-interacting proteins. *SAC1–SAC5* yield recessive suppressors (Novick et al., 1989; Cleves et al., 1989) while *SAC6* yields dominant suppressors of *actl-1* (Adams and Botstein, 1989). *SAC6* encodes a yeast actin-binding protein (Drubin et al., 1988; Adams et al., 1989) functionally and structurally related to the actin-bundling proteins fimbrin and plastin (Adams et al., 1991).

actl-1 and *actl-2* mutants are Osm^S in addition to Ts (Novick and Botstein, 1985). Suppressor mutations in *SAC1* (Novick et al., 1989) revert only the Ts phenotype and not the Osm^S phenotype of *actl-1* (D. Botstein, personal communication). To identify genes whose products functionally interact with actin in cellular responses to osmotic stress, we have isolated extragenic suppressors which revert only the Osm^S but not the Ts phenotype of an *actl-1* mutant. These suppressors identify three genes, *RAH1–RAH3* (*r*eversion of *a*ct1 *h*igh osmolarity *s*ensitivity). Morphological and genetic analysis of a mutation in the *RAH3* gene suggests that the product of this gene is an actin-binding protein that allows recovery of actin filament organization following osmotic stress. These results introduce "phenotype-specific suppression" as a method for identifying genes whose products interact with multifunctional cytoskeletal proteins such as actin.

Materials and Methods

Genetics

Genotypes of haploid and diploid yeast strains used are in Table I. YEPD media contained 1% yeast extract, 2% bactopeptone, and 2% dextrose. Osmotic sensitivity was tested on YEPD agar plates containing 900 mM NaCl (NaCl plates), 1.2 M KCl (KCl plates), or 1.8 M sorbitol (sorbitol plates). Cells were routinely grown at room temperature for all experiments except when testing for temperature-sensitive growth. Complementation testing and tetrad analysis was performed as described by Sherman et al. (1983). Construction of double mutants was confirmed by backcrossing to wild-type (DBY877 or DBY2057). The prototrophic tetraploid strain SCY10 was constructed by crossing HK1 with H111 and picking a zygote by micromanipulation.

To isolate independent osmoresistant (Osm^R) revertants of an *actl-1* mutant, 150 colonies of DBY1691 and 40 of SCY6 were grown separately at room temperature overnight in liquid YEPD, and each culture spread onto a single NaCl plate. After a 1–2-wk incubation at room temperature, NaCl plates with colonies were replica plated to YEPD and placed at 37°C overnight. Although both Osm^R Ts^+ and Osm^R Ts revertants were found, only the latter group was analyzed further. One Osm^R Ts colony was picked from each NaCl plate, streaked out for single colonies on YEPD, and the phenotypes of the strain rechecked. To determine the degree of temperature sensitivity, revertants were replica-plated to YEPD plates, placed at 37°C overnight, and scored for growth. Strains which failed to grow at this time (e.g., *actl-1*) were labeled Ts. The same plates were then left at room temperature overnight and scored for growth again. A replica-plated patch of *actl-1* mutant cells grew up uniformly after this treatment suggesting that recovery of growth after 37°C treatment was not limited to a few cells but is a property of the majority of the cells in the patch. Other strains which failed to noticeably grow at this time were labeled temperature-sensitive lethal or Ts^L. Cold sensitivity was tested by placing strains on YEPD plates for 7 d at 14°C. Osmotic sensitivity was determined by replica plating to NaCl, KCl, and sorbitol plates and scoring growth after 2 d at room temperature. All of the mutants pursued further grew as well as a wild-type control strain (DBY 877) on each of the three plates; this phenotype is referred to as Osm^R in this paper.

To determine whether suppressor mutations were dominant or recessive, each Ts Osm^R revertant was mated to the *actl-1* mutant DBY1691 (or SCY6), diploids isolated, and tested for both temperature- and osmotic-sensitive growth. Revertants which yielded Osm^S diploids were judged to have recessive suppressor mutations, those yielding Osm^R diploids had dominant suppressors. Complementation testing was done by crossing recessive suppressor-containing strains of opposite mating type and testing the resultant diploids for an Osm^S phenotype. If the diploid was Osm^S, the two haploid mutants complement each other; Osm^R diploids indicated a non-complementing pair of mutants. Except in rare cases, non-complementation is observed when two mutations in the same gene are present in the original haploid strains. Complementation, implied by Osm^S, generally indicates mutations in different genes.

Nine strains containing dominant suppressors were backcrossed to the wild-type stain DBY877 (or DBY2057). Analysis of tetrads from these crosses showed that of the original revertants containing dominant suppressors, four were genetically complex with *actl-1* plus two or more independently sorting mutations, each of which had an effect on the Ts or Osm^R phenotype. These four strains were not studied further. One revertant contained a suppressor tightly linked to *actl-1* which was most likely an intragenic revertant. As described below, the other four revertants proved to be double mutants of *actl-1* and a second unlinked suppressor mutation.

Backcrosses of these four remaining strains to wild-type (DBY877 or DBY2057) yielded the following patterns of phenotypes in the resulting tetrads. The number of each type of tetrad observed is given in parentheses. The SCY7 strain showed three types of tetrads: 2 $TsOsm^R$:2 Ts^+Osm^R (2), 2 $TsOsm^R$:1 $TsOsm^S$:1 Ts^+Osm^R (9), and 2 $TsOsm^R$:2 $TsOsm^S$ (3). The SCY1 strain showed three types of tetrads: 2 Ts^LOsm^R:2 Ts^+Osm^R (7), 1 Ts^LOsm^R:1 $TsOsm^R$:1 $TsOsm^S$:1 Ts^+Osm^R (17), and 2 $TsOsm^R$:2 $TsOsm^S$ (9). The SCY8 strain showed three types of tetrads: 2 Ts^LOsm^R:2 Ts^+Osm^R (2), 1 Ts^LOsm^R:2 $TsOsm^S$:1 Ts^+Osm^R (15), and 4 $TsOsm^S$ (3). The SCY9 strain showed three types of tetrads: 2 $TsOsm^R$:2 Ts^+Osm^R (7), 1 $TsOsm^S$:1 $TsOsm^R$:2 Ts^+Osm^R (22), and 2 Ts^+Osm^R:2 $TsOsm^S$ (3). These data were interpreted as the parental ditype, tetratype, and nonparental ditype expected for backcrosses of four double mutants containing *actl-1* plus a suppressor mutation that also had a Ts phenotype (SCY1 and SCY7), a Ts and an Osm^S phenotype (SCY8), or had no other phenotype (SCY9). Strains containing the suppressor mutation in an *ACT1*$^+$ background were identified as follows. Likely candidates were picked from the non-parental ditype tetrads and crossed with an *actl-1* strain (DBY1691 or SCY6). If the patterns of phenotypes in the resulting tetrads matched that of the original backcross, we concluded that the candidate strain contained the suppressor in an *ACT1*$^+$ background.

Genetic crosses between each of the three Ts mutants in an *ACT1*$^+$ back-

Table I. Yeast Strains Used in This Study

Strains	Genotype	Source
DBY877	*MATα his4-619*	Botstein (Stanford University, Stanford, CA)
DBY2057	*MATa ura3-52*	Botstein
DBY1691	*MATa his4-619 act1-1*	Botstein
DBY1694	*MATa his4-619 act1-2*	Botstein
DBY5218	*MATa ura3-52 act1-1 tub2-201 sac6-6*	Botstein
HK1	*MATa/MATa lys1-1/lys1-1*	Fink (MIT, Cambridge, MA)
H111	*MATα/MATα ade5/ade5 lys2/lys2 ino1/ino1 ino4/ino4*	Culbertson (University of Wisconsin, Madison, WI)
SCY1	*MATa his4-619 act1-1 rah3-2*	This study
SCY2	*MATα ura3-52 at1-1 rah3-2*	This study
SCY3	*MATα ura3-52 rah3-2*	This study
SCY4	*MATa ura3-52 rah3-2*	This study
SCY5	*MATα his4-619 rah3-2*	This study
SCY6	*MATα ura3-52 act1-1*	This study
SCY7	*MATα ura3-52 act1-1 rah3-1*	This study
SCY8	*MATa ura3-52 act1-1 rah3-3*	This study
SCY9	*MATα ura3-52 act1-1 rah3-4*	This study
KSY1	*MATα ura3-52 rah3-1*	This study
KSY2	*MATα ura3-52 rah3-3*	This study

ground yielded only 4 Ts:0 Ts^+ tetrads. This data, indicating tight linkage, suggested that the three mutations are allelic. To test for genetic linkage between the dominant extragenic suppressor with no phenotype in an *ACT1*$^+$ background and these three mutations, the original revertants were mated with each other, diploids sporulated, and the progeny tested for osmotic-sensitive growth. All tetrads in each of the crosses segregated as 4 Osm^R:0 Osm^S showing that all four dominant extragenic suppressors are tightly linked to each other. In contrast, crosses between the dominant extragenic suppressor strains and strains containing representative suppressor alleles of the *RAH1* or *RAH2* complementation group, all in an *act1-1* background, yielded a mixture of 4 Osm^R:0 Osm^S, 3 Osm^R:1 Osm^S, and 2 Osm^R:2 Osm^S tetrads. This segregation pattern is that expected for unlinked suppressor mutations.

Growth Curves and Drop Tests

For growth curves, cultures were first grown to log phase at room temperature in liquid YEPD. The culture density was determined using the absorbance at 600 nm for the first time point (t = 0). This initial density was subtracted from subsequent culture densities to determine the actual change in culture density due to osmotic stress. The osmolarity of the culture was then shifted by the addition of a 4× volume of YEPD (control) or YEPD plus 500 mM NaCl or 750 mM glucose. Aliquots of the culture were removed at different times and the culture density determined using the absorbance at 600 nm. For drop tests, each strain was grown to log phase and the cell density determined using a hemocytometer. The cell density was then adjusted to 10^7 cells/ml and 10 μl of this suspension spotted on an agar plate for testing of growth under the conditions indicated.

Fluorescence Microscopy

Fluorescent staining of cells under various osmotic stresses was accomplished by the following protocol. Yeast cultures were grown to log phase in liquid YEPD. One ml of the culture was then mixed by vortexing with 4 ml of YEPD or YEPD plus 0.75 M glucose, 0.95 M glycerol, 0.75 M KCl, 0.5 M NaCl, or 0.9 M sorbitol. Since centrifugation alone was observed to alter actin distribution in cells, centrifugation of the cells immediately before or during a change in media osmolarity was avoided. After incubating for the indicated times at room temperature, the cells were fixed by adding formaldehyde (final concentration of 4%) or 0.1 mM m-maleimidobenzoyl-*N*-hydroxysuccinamide ester (MBS; Pierce Chemical Co., Rockford, IL) plus 0.05% Triton X-100 (Sonobe and Shibaoka, 1989) directly to the culture. After 30 min of fixation at room temperature, cells were pelleted and resuspended in 35 mM potassium phosphate (pH 6.8), 0.5 mM $MgCl_2$, plus 4% formaldehyde. After two more hours of fixation, cells were washed twice in PBS and then stained with rhodamine–phalloidin (Rh-phalloidin; Molecular Probes Inc., Junction City, OR) at a final concentration of 0.3 μM for 90 min (Adams and Pringle, 1991). Staining of cell wall chitin was achieved using Calcofluor as described by Novick and Botstein (1985). After staining, cells were washed twice in PBS and suspended in mounting media: 1 g of *p*-phenylenediamine dissolved in 30 ml PBS to which 70 ml of glycerol was added (Johnson and de C. Nogueira Araujo, 1981). To reduce Brownian motion during photomicroscopy, 1.7 μl of stained cells in mounting media was spotted onto a regular glass slide, a coverslip placed over it, and then tapped lightly. Film used for taking fluorescence microscopy pictures was T-MAX 100 (Eastman Kodak Co., Rochester, NY).

Results

Osmotic Stress Causes the Reversible Disassembly of the Actin Cytoskeleton

To analyze the effect of osmotic stress on actin in yeast cells, a log phase yeast culture was subjected to a step increase in external osmolarity, the cells fixed rapidly by direct addition of formaldehyde to the media, and the actin distribution in cells analyzed by fluorescence microscopy. Rh-phalloidin, which preferentially stains filamentous actin (Wulf et al., 1979; Cooper, 1987), was used to visualize actin filaments in the fixed cells. A tetraploid strain, SCY10, was constructed (see Materials and Methods) and used for these experiments. Although similar results were obtained with haploid and diploid cells, the larger cell diameter of SCY10 made it easier to visualize actin filaments. The effect of increasing external osmolarity on actin filaments was most obvious in cells about to bud or those with small buds. In the mock-treated control cells (Fig. 1 *a*), actin filament distribution was identical to that described by others (Adams and Pringle, 1984; Kilmartin and Adams, 1984), i.e., actin filament cables of varying diameter in mother cells oriented toward the nascent bud and cortical patches of actin filaments in small-budded cells localized almost exclusively to the bud. When the external osmolarity was raised using 0.6 M glucose, the localization of filamentous actin changed over time. Within the first minute after a step increase in external osmolarity, actin filament cables disappeared from the mother cell (Fig. 1 *b*). Over the next 30 min, cortical actin filament patches delocalized from the daughter cell to the mother cell (Fig. 1 *c*). All of these changes were reversible. After 1–2 h, the cellular location of Rh-phalloidin–stained actin in osmotically stressed cells (Fig. 1 *d*) had been restored to that seen in the mock-treated control cells. Earlier

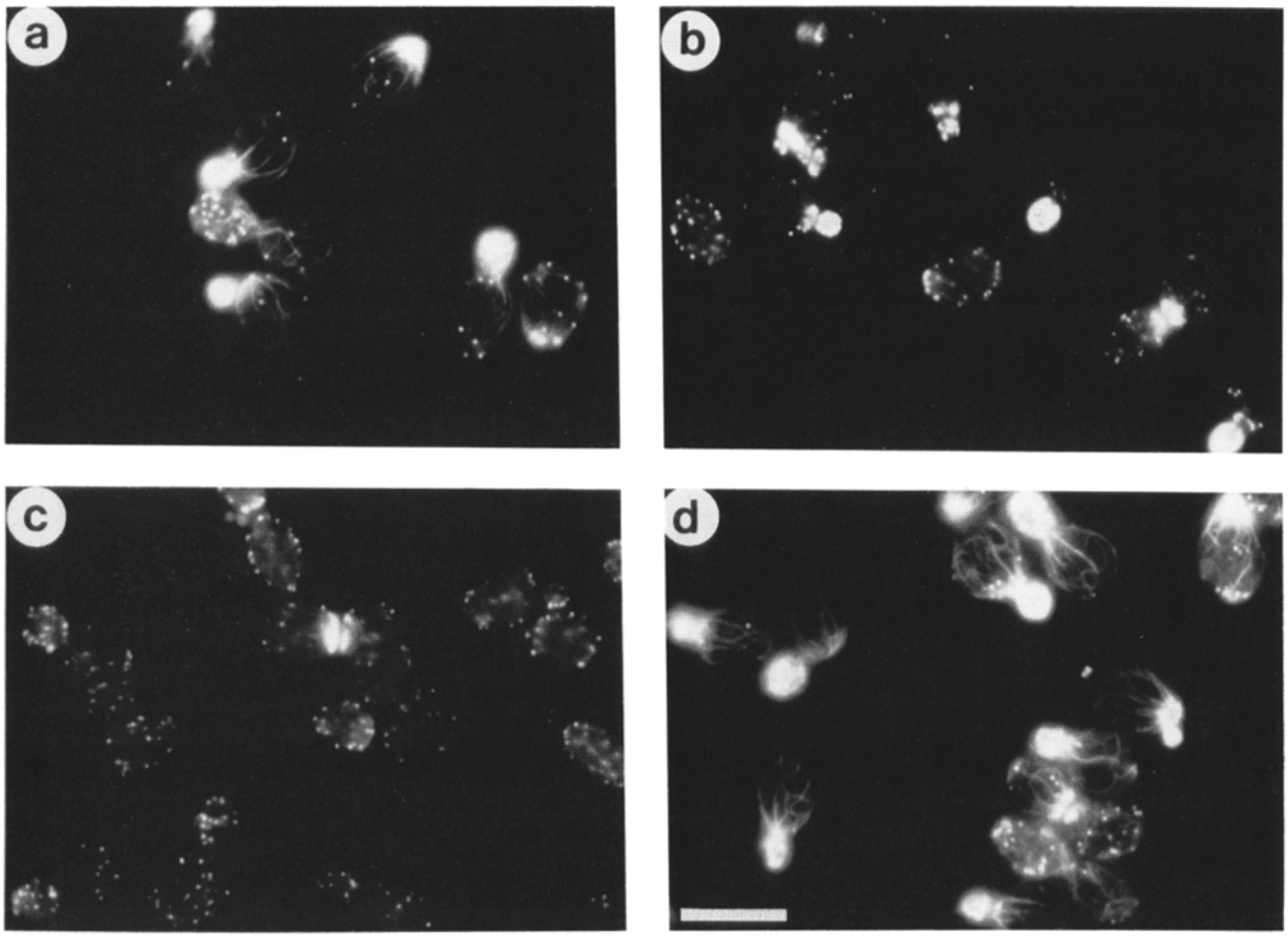

Figure 1. Actin filament localization in wild-type cells upon exposure to osmotic stress. Log phase cells (*SCY10*) were grown in YEPD and then (*a*) shifted to YEPD or shifted to YEPD plus 0.6 M glucose for (*b*) 1 min, (*c*) 30 min, or (*d*) 1 h. Cells were fixed and stained with Rh-phalloidin as described in Materials and Methods. Control experiments were performed to attempt to rule out fixation artifacts. Increasing osmolarity after fixation had no effect on actin filament organization in control cells. The distribution of actin filaments in control and osmotically-stressed cells was the same whether cells were fixed with formaldehyde (final concentration = 1 M) or with a different cross-linking agent, m-maleimidobenzoyl-*N*-hydroxysuccinamide ester (final concentration = 0.1 mM) (Sonobe and Shibaoka, 1989). Bar, 10 μm.

studies by Novick et al. (1989) had shown that starvation for glucose caused disassembly of the actin cytoskeleton in yeast. The changes observed here occurred in media containing excess glucose, arguing against effects due to nutrient deprivation.

If these changes reflect a response to a change in external osmolarity, then raising the osmolarity with other solutes ought to induce similar alterations in actin filament distribution. The results of the experiments shown in Fig. 2 confirm this prediction. The characteristic pattern of actin staining observed in mock-treated control cells (Fig. 2 *a*), was disrupted in cells exposed to elevated concentrations of several different solutes, including glucose (Fig. 2 *b*), glycerol (Fig. 2 *c*), KCl (Fig. 2 *d*), NaCl (Fig. 2 *e*), and sorbitol (Fig. 2 *f*) for 15 min. Each solute had roughly similar effects on the actin cytoskeleton, causing loss of cables and redistribution of cortical actin patches to the mother cell.

Analysis of the distribution of cortical actin filament patches in the larger mother cells was difficult in photographs because the focal plane for each cell catches only a fraction of the cortical patches. To determine more accurately the effect of osmotic stress on the number of patches in mother cells, we counted patches in individual cells under the microscope, moving the focus up and down. Only those cells in which the bud was less than half the size of the mother cell were analyzed. The numerical distribution of mother cells with 0, 1, 2, or more patches is shown for a culture of wild-type haploid cells (DBY877) in YEPD for 30 min (Fig. 3 *a*) or 30 sec (Fig. 3 *b*) and 30 min (Fig. 3 *c*) after addition of YEPD plus 0.4 M NaCl. These results show that osmotic stress caused a slow increase in patch accumulation in the mother cell. Because counting the densely packed patches in small buds of the control cells was difficult, we do not know whether the overall number of patches in budded cells changes after osmotic stress.

Shifting log phase cells from YEPD to YEPD plus either 0.6 M glucose or 0.4 M NaCl cause a temporary pause in cell growth (Fig. 4). Although approximately equimolal activities of glucose and NaCl were used in this experiment, the lag before continuation of growth was longer for NaCl. The length of the lag period before recovery of normal actin filament distribution following osmotic stress was roughly correlated to the different lag periods in cell growth observed for NaCl and glucose.

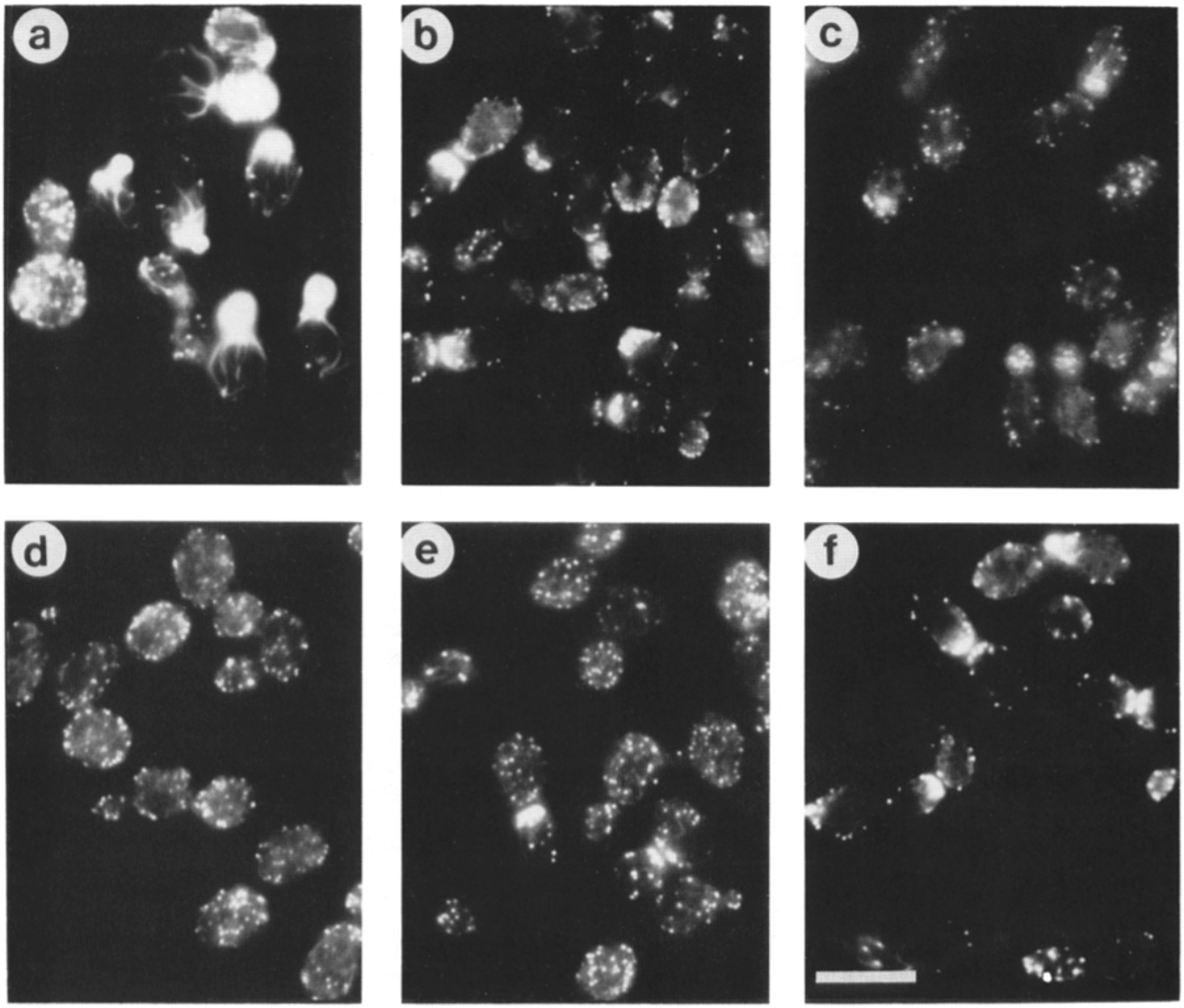

Figure 2. Distribution of actin filaments in wild-type cells after exposure to osmotic stress using different solutes. Log-phase cells (*SCY10*) were exposed to (*a*) YEPD or YEPD plus (*b*) 0.6 M glucose, (*c*) 0.76 M glycerol, (*d*) 0.6 M KCl, (*e*) 0.4 M NaCl, or (*f*) 0.72 M sorbitol for 15 min. Cells were fixed and stained with Rh-phalloidin as described in Materials and Methods. Bar, 10 μm.

Isolation of Phenotype-specific Suppressors of an Actin Mutant

The temporal correlation between the alterations in actin filament organization and the pause in cell growth following osmotic stress suggested a model to explain the osmotic-sensitive phenotype of actin mutants. In this model, the reversible disassembly of the actin cytoskeleton, defective in the actin mutants (see below), is required for adaptation to increased external osmolarity and resumption of cell growth. One prediction of this model is that genes encoding actin-interacting proteins required for this osmotic stress response exist. Moreover, such genes ought to yield mutations that suppress the Osm^S phenotype of an actin mutant. Among such mutations would be those that have exactly the opposite profile of known mutations in *SAC1* genes which suppress the Ts but not the Osm^S phenotype of actin mutations (D. Botstein, personal communication). We therefore sought mutations genetically unlinked to *act1-1* which suppress its Osm^S but not its Ts phenotype. Anticipated in this study were both recessive mutations which bypass the need for wild-type actin in high osmolarity media and dominant mutations that identify potential actin-binding protein genes. Although both were obtained, we confined our initial analysis to the latter class of mutations.

Phenotype-specific suppressors of *act1-1* were isolated by selecting Osm^R revertants of *act1-1* (DBY1691 or SCY6) on NaCl plates and then screening for retention of the *act1-1* Ts defect (see Materials and Methods). 65 Ts Osm^R strains were isolated. Many of these strains (21/65) had a stronger Ts phenotype than the original *act1-1* mutant and were termed Ts^L for temperature-sensitive lethal to distinguish it from that of the original *act1-1* strains (see Materials and Methods). 56 of the Osm^RTs or Osm^RTs^L revertants contained recessive suppressors. The recessive mutations formed at least two complementation groups containing 35 and 3 alleles, respectively. Crosses between representative alleles of the two complementation groups showed that they are unlinked, identifying two genes *RAH1* and *RAH2*, respectively (*RAH*, *r*eversion of *a*ct1 *h*igh osmolarity sensitivity). Of nine strains containing dominant suppressors, four were genetically complex, one contained a suppressor

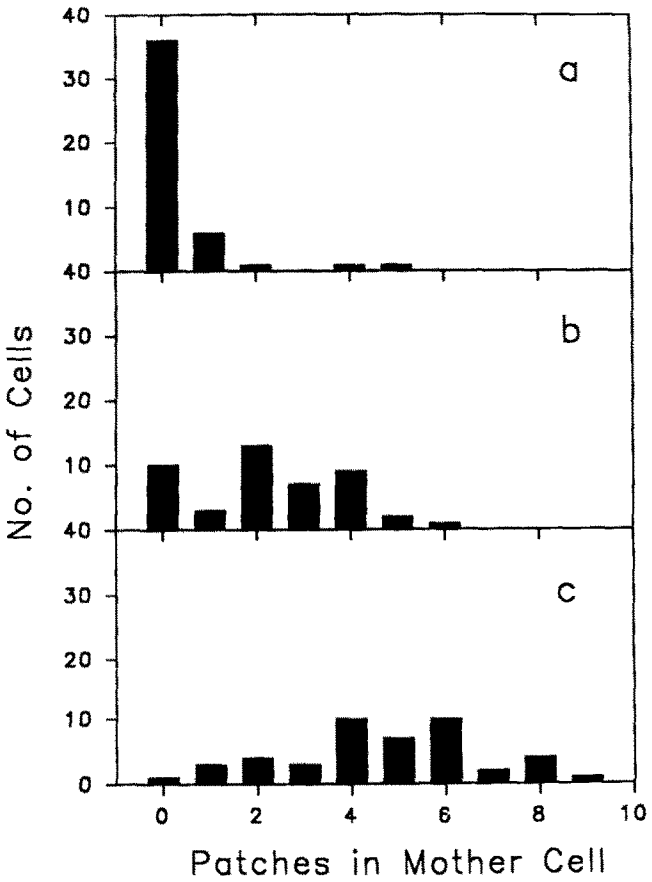

Figure 3. Distribution of cortical actin patches in yeast cells after osmotic stress. Log-phase cells (*DBY877*) were grown in (*a*) YEPD for 30 min, (*b*) YEPD plus 0.4 M NaCl for 30 s, or (*c*) YEPD plus 0.4 M NaCl for 30 min. Cells were then fixed and stained with Rh-phalloidin as described in Materials and Methods.

linked to *act1-1*, and four contained a single suppressor mutation unlinked to *act1-1* (see Materials and Methods). In genetic crosses, each of the latter four mutations was tightly linked to each other, but unlinked to *rah1* or *rah2* suppressor

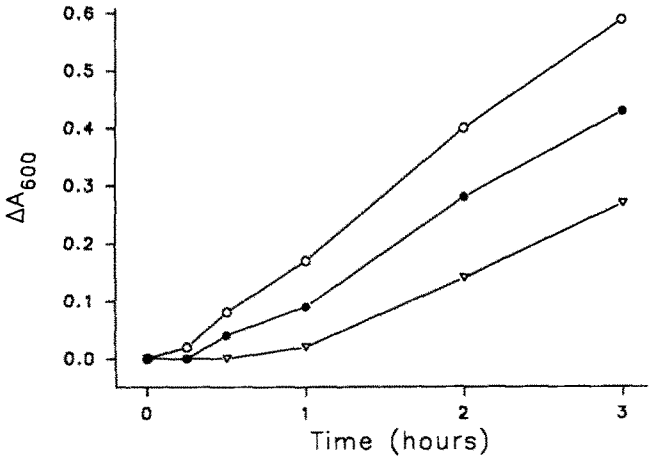

Figure 4. Growth rates of log phase wild-type cells (*DBY877*) in -○- YEPD, -●-YEPD plus 0.6 M glucose, or -▽- YEPD plus 0.4 M NaCl measured by optical density at 600 nm as described in Materials and Methods.

mutations. These four dominant suppressors are therefore alleles of a third gene, *RAH3*. Thus, three genes, *RAH1–RAH3*, are capable of yielding mutations which suppress only the Osm^S phenotype of *act1-1*.

Dominant Suppressors of an Osm^S Actin Mutant

Three suppressor mutations in *RAH3*, *rah3-1*, *rah3-2*, and *rah3-3*, had a conditional growth phenotype in an *ACT1*$^+$ background; one, *rah3-4*, did not (see Materials and Methods). All of the dominant extragenic suppressors of the Ts *act1-1* isolated by Adams and Botstein (1989) were mutations in *SAC6*, a gene identified as encoding an actin-binding protein. Three *sac6* mutations isolated using this approach have a conditional growth phenotype (Ts) in an *ACT1*$^+$ background. Therefore, to focus on mutations most likely to identify potential actin-binding protein genes, the *rah3* mutants were chosen for more complete characterization. *ACT1*$^+$ strains containing a *rah3-1*, *rah3-2*, or *rah3-3* mutation were Ts, failing to grow at elevated temperature. None of the three strains were cold sensitive. In a cross with wild-type (DBY877 or DBY2057), the Ts phenotype of each mutant segregated 2 mutant:2 wild-type in 10/10 tetrads (*rah3-1*), 53/59 tetrads (*rad3-2*), and 16/16 tetrads (*rah3-3*), suggesting in each case that a single gene mutation was responsible for the Ts phenotypes. The *rah3-1* mutant was weakly Ts at 37°C but strongly Ts at 39°C; the *rah3-2* mutant was strongly Ts at 37°C. Both mutants were Osm^R. Raising the osmolarity of the media did not suppress the Ts phenotype of *rah3-1* and *rah3-2*. The Ts phenotypes of both mutations were recessive. The *rah3-3* mutation in an *ACT1*$^+$ background was Ts at 37°C and Osm^S at the permissive temperature. The Ts and Osm^S phenotypes co-segregated in all 16 tetrads from the cross of *rah3-3* (KSY2) with wild-type (DBY877), indicating both phenotypes are very likely the result of the same mutation. The Ts phenotype of *rah3-3* was recessive to the wild-type allele while the osmotic sensitivity of the heterozygous diploids (*rah3-3*/+) was less than that of a *rah3-3*/*rah3-3* diploid but greater than that of a wild-type diploid. The Osm^S phenotype of *rah3-3* was therefore semi-dominant to wild-type. *rah3-1*, *rah3-2*, and *rah3-3* failed to complement each other's Ts phenotypes, consistent with all three mutations occurring in the same gene. To confirm that the *rah3* alleles with a conditional growth phenotype were suppressors of *act1-1*, *rah3-1*, *rah3-2*, and *rah3-3* mutants were each crossed with an *act1-1* mutant (DBY1691 or SCY6). In each case, the segregation of conditional growth phenotypes in the resulting tetrads was that predicted for the *rah3* mutants acting as phenotype-specific suppressors of the Osm^S phenotype of *act1-1* (see Materials and Methods). A *rah3-2* mutant (SCY3) was transformed with plasmid containing either the cloned *SAC6* (Adams and Botstein, 1989), *PFY1* (Haarer et al., 1990), *CAP2* (Amatruda et al., 1990), *TPM1* (Liu and Bretscher, 1989), *ABP1* (Drubin et al., 1988), or *SAC7* (Dunn and Shortle, 1990) gene. Each of these genes failed to complement the Ts defect of *rah3-2* (not shown). *RAH3* is therefore a different gene from each of these known actin-binding genes.

Genetic Evidence for Physical Interaction between the RAH3 Gene Product and Actin

From this collection of mutants, we chose to study *rah3-2*

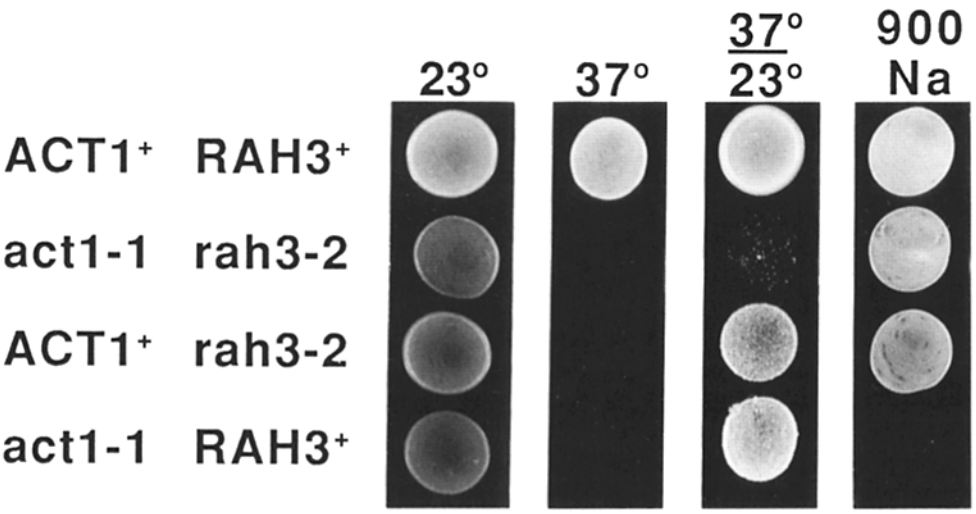

Figure 5. Growth of wild-type (*DBY877*) and mutant cells (*SCY1*, *SCY3*, and *DBY1691*) on YEPD at room temperature (23°C), high temperature (37°C), recovery from high temperature (37°C/23°C), and after osmotic stress (YEPD plus 0.9 M NaCl). To control for differences in genetic background, several strains for each type of mutant were tested. Data shown is representative of the growth phenotype observed for each type of mutant.

in greater detail. The growth of four strains, an *act1-1* mutant (DBY1691), a *rah3-2* mutant (SCY5), an *act1-1 rah3-2* double mutant (SCY1), and a wild-type strain (DBY877), were compared under several conditions. Equal numbers of cells from each strain were spotted on one of four different plates and allowed to grow at a permissive condition (YEPD, 23°C), at elevated temperature (YEPD, 37°C), at elevated temperature followed by recovery at permissive temperature (YEPD, 37°C/23°C), and at high osmolarity and permissive temperature (YEPD plus 900 mM NaCl, 23°C). As shown in Fig. 5, all three mutant strains failed to grow at 37°C. The *act1-1* mutant failed to grow on the NaCl plate. The *rah3-2* mutation affected both conditional growth phenotypes of *act1-1*, enhancing its Ts phenotype from Ts to Ts^L and suppressing its Osm^S phenotype. The Ts enhancement effect was observed on the 37°C plate where cells were allowed to recover and grow at 23°C.

A *rah3-2*/+ *act1-1*/*act1-1* diploid was both Ts^L and Osm^R (Table II), demonstrating that both the Ts enhancement and Osm^S suppression phenotypes of *rah3-2* were dominant. A *rah3-2*/*rah3-2*, *act1-1*/+ diploid was also Ts^L. Thus, *act1-1* and *rah3-2*, each of which confers a recessive Ts phenotype, demonstrated dominant reciprocal enhancement of each other's Ts phenotype. This genetic data provides strong support for a physical interaction between the products of these two mutant genes which apparently allows cell growth at high osmolarity but not at elevated temperatures. By extrapolation, these observations also suggest that specific physical interactions between the products of two wild-type genes, *ACT1*$^+$ and *RAH3*$^+$, are required for growth-related functions of the actin cytoskeleton. Two additional observations support this hypothesis. First, a cross between *rah3-2* and *act1-2* strains revealed that the *rah3-2 act1-2* double mutant was inviable even at room temperature. This data suggests allele-specific interactions between *RAH3* and *ACT1*, a characteristic expected for physically interacting gene products. Second, *rah3-2* cells had an aberrant actin cytoskeleton at both permissive and non-permissive temperatures (see below).

As previously discussed, *act1-1* and *rah3-2* enhanced each other's Ts phenotype. For each mutation, the Ts enhancement phenotype was dominant to that of the wild-type allele. These data suggest a preferential association of mutant proteins with each other rather than with the wild-type protein. To determine whether this putative complex of mutant proteins can interfere with the function of the wild-type gene products, an *act1-1*/+ *rah3-2*/+ diploid was constructed and tested for growth at 37°C (Table II). The phenotype of this heterozygous diploid was Ts^+ indicating that wild-type actin and the wild-type *RAH3* gene product can functionally interact despite the presence in the same cell of the *act1-1* and *rah3-2* gene products.

Table II. Phenotypic Analysis of Mutant Diploids

Genotype	37°	900 mM Na
act1-1 / *act1-1* *	−	−
rah3-2 / *rah3-2* ‡	−	+
act1-1 / + §	+	+
rah3-2 / + ‖	+	+
rah3-2 act1-1 / + *act1-1* ¶	lethal	+
rah3-2 act1-1 / *rah3-2* + **	lethal	+
rah3-2 act1-1 / *rah3-2 act1-1* ‡‡	lethal	+
rah3-2 act1-1 / + + §§	+	+

Diploid strains were isolated after mating between appropriate strains and their growth phenotypes determined as described in Materials and Methods. Wild-type growth at 37°C or on YEPD plus 900 mM NaCl was defined as "+." The criteria distinguishing Ts (−), from Ts^L (*lethal*) are given in Materials and Methods.

* Constructed by mating DBY1691 with SCY6.
‡ Constructed by mating SCY4 with SCY5.
§ Constructed by mating DBY1692 with DBY2057.
‖ Constructed by mating SCY5 with DBY2057.
¶ Constructed by mating DBY1691 with SCY2.
** Constructed by mating SCY1 with SCY3.
‡‡ Constructed by mating SCY1 with SCY2.
§§ Constructed by mating DBY1691 with SCY3.

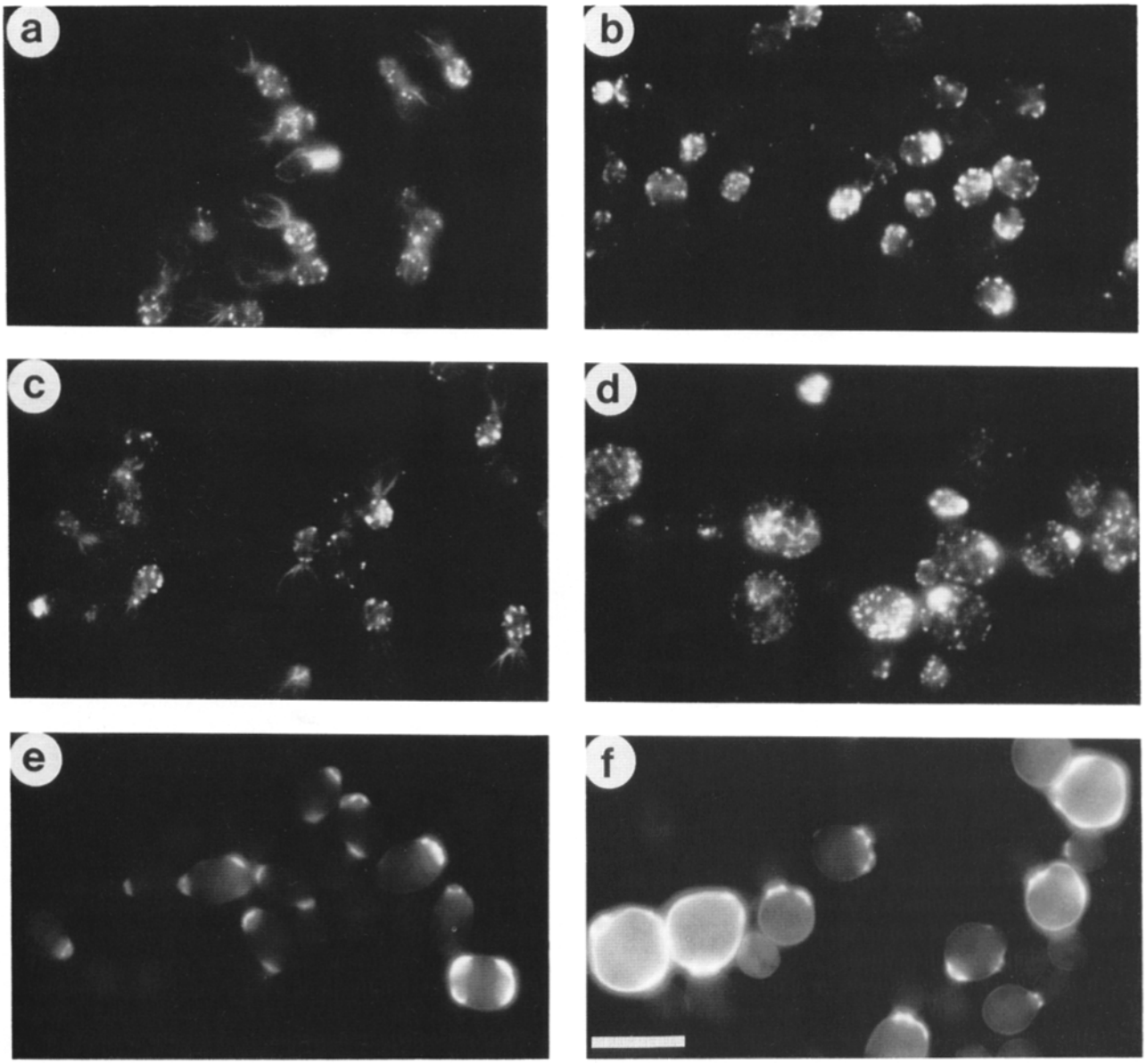

Figure 6. Fluorescent localization of actin in diploid wild-type and *rah3-2* cells. Log phase cells were grown at room temperature (*a* and *b*) and then shifted to YEPD at 37°C for 1 h (*c–f*). Cells were then stained with Rh-phalloidin (*a–d*) or Calcofluor (*e* and *f*) as described in Materials and Methods. The wild-type strain was constructed by crossing DBY877 with DBY2057, while the *rah3-2* homozygous mutant strain was from a cross of SCY4 with SCY5. Bar, 10 μm.

A Mutation in RAH3 Changes the Organization of the Actin Cytoskeleton

Our genetic data suggest that the gene product of the *rah3-2* allele interacts with a mutant actin, the product of the *act1-1* allele. This finding predicts that *RAH3* might encode an essential component of the yeast cytoskeleton. Furthermore, the ability of *rah3-2* to suppress the Osm^s phenotype of *act1-1* predicted a possible role for *RAH3* in the response of the actin cytoskeleton to osmotic stress. We therefore microscopically examined *rah3-2* cells, comparing them to wild-type cells. Log-phase cells were exposed to either elevated temperature (37°C) or high osmolarity (0.4 M NaCl) for various times, fixed with formaldehyde, washed in PBS, and then stained for actin filaments using Rh-phalloidin or for cell wall chitin using Calcofluor. At room temperature, *rah3-2* cells (Fig. 6 *b*) exhibited a lack of the actin cables seen in the wild-type control cells (Fig. 6 *a*). However, cortical patch distribution was similar between the two cell types. When shifted to 37°C for 1 h, the normal distribution of actin filaments in the wild-type cells (Fig. 6c), was clearly aberrant in the *rah3-2* cells (Fig. 6 *D*). Instead of patches of actin filaments localized to the emerging bud, the staining pattern in *rah3-2* cells showed heavy concentrations of actin staining in several locations in the mother cell. This pattern was also observed in *rah3-2 act1-1* cells at 37°C (data not shown). Also, *rah3-2* cells were enlarged relative to the wild-type cells, reminiscent of *act1-1* cells (Novick and Botstein, 1985). Experiments with the *rah3-1* and *rah3-3* strains also exhibited similar changes in actin localization (data not shown). Staining of cells with the chitin-specific fluorescent probe Calcofluor, showed delocalized chitin staining on the surface of mother cells for the *rah3-2* mutant (Fig. 6 *f*) but not wild-type (Fig. 6 *e*). Mutations in actin cytoskeleton

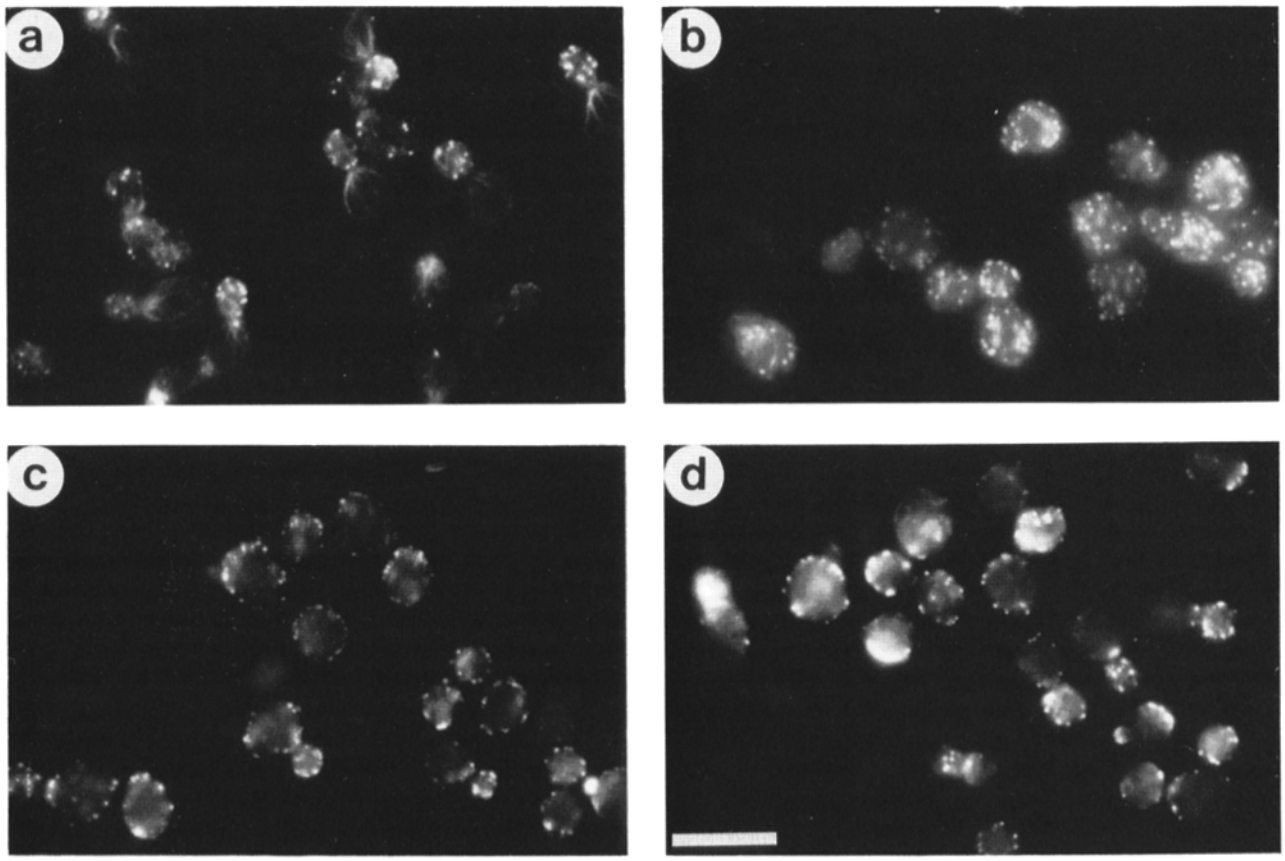

Figure 7. Localization of actin filaments in wild-type and *rah3-2* mutants after long term exposure to osmotic stress. Log phase (*a*) wild-type, (*b*) *act1-1*, (*c*) *rah3-2 act 1-1*, or (*d*) *rah3-2* diploid cells were grown in YEPD and then switched to YEPD plus 0.4 M NaCl for 4 h. Strain construction for *a* and *b* has been described in Fig. 6. The *rah3-2 act1-1* homozygous double mutant strain (*c*) was from a cross of SCY1 with SCY2 while the *act1-1* homozygous mutant strain (*d*) was derived from a cross of DBY1691 with SCY6. Bar, 10 μm.

genes such as those encoding tropomyosin (*TPM1*; Liu and Bretscher, 1989), myosin (*MYO1*; Rodriguez and Paterson, 1990), profilin (*PFY1*; Haarer et al., 1990) or an actin filament capping protein (*CAP2*; Amatruda et al., 1990) result in this same characteristic combination of morphological phenotypes in growing cells: defects in actin filament organization, delocalization of chitin on the cell surface, and cell enlargement. Thus, these data are consistent with *RAH3* encoding an essential component of the actin cytoskeleton in yeast.

When each of these four strains was exposed to YEPD containing 0.4 M NaCl, the greatest differences in actin filament distribution (revealed by staining with Rh-phalloidin) were observed after 4 h. The recovery-associated redistribution of cortical actin filament patches to small buds following osmotic stress was observed in the wild-type (Fig. 7 *a*), to a lesser extent in *rah3-2* and *rah3-2 act1-1* strains (Fig. 7, *c* and *d*), but rarely in the *act1-1* strain (Fig. 7 *b*). Actin filament cables were only rarely observed in the mutant strains. Thus, the ability of *rah3-2* to allow *act1-1* cells to recover from osmotic stress was correlated with restoration of an asymmetric distribution of cortical actin filament patches following osmotic stress.

Discussion

We report here the discovery and characterization of a novel physiological response of the actin cytoskeleton in yeast: the rapid and reversible disassembly of the actin cytoskeleton in response to osmotic stress. We have also successfully applied a variation of the suppressor approach for isolating mutations in genes whose products functionally interact with actin: isolation of phenotype-specific suppressors. Morphological and genetic properties of one of these mutations suggests that the product of the wild-type gene, *RAH3*$^+$, is an actin-binding protein that interacts with actin to allow reassembly of the cytoskeleton following osmotic stress.

Diploid yeast with just one copy of *ACT1* are Osm^s (see D. Shortle communication cited in Novick and Botstein, 1985). This observation suggests that some underlying growth-related process involving the actin cytoskeleton is osmosensitive. In general, the level of gene expression in yeast is proportional to the number of copies of a gene (Rine, 1990). Halving the number of *ACT1* genes is therefore likely to reduce the concentration of actin in yeast. Assuming that the polymerization of actin into filaments depends on the concentration of actin monomers, the Osm^s phenotype of a diploid with one *ACT1* could be explained by an osmotic stress–induced shift of the actin monomer–polymer equilibrium toward actin depolymerization. Recovery from this response would require the re-polymerization of actin. We observe that actin filament cables are rapidly lost in osmotically-stressed cells and then restored at a later time (Fig. 1). The number of cortical actin filament patches in the buds of small-budded cells first decreases and then increases following osmotic stress. These data are consistent with an osmotic

stress-induced cycle of actin depolymerization and repolymerization, but other mechanisms such as actin filament redistribution cannot be ruled out.

The organization of actin filaments in yeast cells is sensitive to a variety of stresses besides osmotic stress (Novick et al., 1989). We have also found that actin filament cables and patches in wild-type cells were sensitive to centrifugation of the cells or to raising the temperature of the media (S. Chowdhury, unpublished results). Other investigators have noted that changing the media also causes changes in actin distribution in yeast cells (Fig. 1, Pringle et al., 1989). Whether the sensitivity of the yeast actin cytoskeleton to a variety of stresses reflects a common mechanism is not known. Why have we focused on the response to osmotic stress per se? There are two reasons. First, simple observation suggests that osmotic stress is physiologically meaningful for yeast. Consider the yeast cell growing on a dehydrating grape in the sun or in the high sugar concentrations at the beginning of a fermentation. Yeast cells can tolerate steps in NaCl concentration up to 0.4 M (or up to 1.4 M when that plateau is approached gradually) without changes in cell viability (Blomberg and Adler, 1989). Second, normal actin function is required for yeast cells to grow in high osmolarity media. This suggests a special relationship between the actin cytoskeleton and cellular responses to osmotic stress.

The isolation of mutations that suppress only the Osm^S phenotype and not the Ts phenotype of an actin mutant has allowed us to begin to determine what other proteins are required for this response to osmotic stress. Actin and tubulin are multifunctional proteins, required for a wide variety of normal cellular processes including responses to specific environmental signals. We anticipate that phenotype-specific suppression of actin or tubulin mutants will be a useful tool for identifying genes coding for actin-binding proteins or microtubule-associated proteins required for specific cell processes involving actin or tubulin. Using this approach, we have identified three genes *RAH1–RAH3*.

Genetic and morphological studies reported here suggest strongly that actin physically interacts with the product of the *RAH3* gene. Key observations in support of this hypothesis are the following. First, like mutations in *SAC6*, a known actin-binding protein (Adams and Botstein, 1989); three *rah3* mutations which have a recessive conditional growth phenotype are also dominant suppressors of a actin mutant. Second *rah3-2* and *act1-1* show dominant reciprocal enhancement of each other's Ts phenotype. Third, the *rah3-2* mutant shows a change in the organization of the actin cytoskeleton, delocalization of chitin on the cell surface, and enlarged cells, all properties shared by mutations in actin cytoskeleton genes. Finally, the *rah3-2* mutation allows an *act1-1* strain to restore cortical actin patches to the bud following an increase in external osmolarity, suggesting an explanation for the suppression of the Osm^S *act1-1* by *rah3-2*. The dominant nature of the suppression by *rah3-2* suggests that the complex of *act1-1* by *rah3-2*. The dominant nature of the suppression by *rah3-2* suggests that the complex of *act1-1* actin and *rah3-2* protein is active in allowing cells to grow at high osmolarity. However, the same logic suggests that this complex is defective for cells trying to grow at elevated temperature. This exacerbation of the *act1-1* Ts phenotype by certain suppressors could reflect a changing association of proteins bound to actin. Cell growth in specific conditions such as high or low temperature may require specific associations between actin and a subset of actin-binding proteins (Novick et al., 1989; Dunn and Shortle, 1990; Adams et al., 1991). The exacerbation of the *act1-1* Ts phenotype observed in certain Osm^R revertants may reflect a competition for actin between a mutant actin-binding protein (the *rah* protein) and a second protein (the *SAC6* protein) required for growth at elevated temperature.

What is the physiological function of the actin cytoskeleton in the response to osmotic stress? One possible function is the cellular coordination of two different processes required for bud growth: delivery of macromolecules to the bud, directed by the actin cytoskeleton, and entry of water, driven by the osmotic gradient. Yeast cells maintain an osmotic gradient across their cell membrane (Brown, 1978). If the osmolarity of the external milieu is increased by the addition of NaCl, the osmotic gradient will be restored by the accumulation of intracellular glycerol up to molar levels (Reeds et al., 1987). Since mutants defective in glycerol accumulation are Osm^S (Brewster et al., unpublished results), restoration of the osmotic gradient is necessary for growth in high osmolarity media. We note parenthetically that the Osm^S phenotype of the *act1-1* is not due to a defect in osmotic stress-induced glycerol accumulation (data not shown). Recovery of actin filament organization in cells following addition of 0.4 M NaCl to the media required approximately 1 h, the time necessary for maximal accumulation of glycerol in similarly treated cells (Brewster et al., unpublished results). This temporal correlation is consistent with collapse of the osmotic gradient as the stimulus for disassembly of the actin cytoskeleton.

Growing cells increase in cell volume, a process requiring an osmotic gradient to drive the entry of water (Dale and Sutcliffe, 1986). Where a cell wall impedes growth such as in plants and fungi, large osmotic gradients create turgor pressure needed to force expansion of the cell wall (Cosgrove, 1986; Ortega et al., 1989). As shown in Fig. 4, yeast cells temporarily stopped growing when the osmotic gradient was experimentally collapsed. We suggest that the water entry-driven expansion of the bud is coordinated with delivery of cellular materials to the bud, catalyzed in part by the actin cytoskeleton. Continued delivery of new materials to the growing bud in the absence of an osmotic gradient to allow cell expansion may be detrimental to the cell. Therefore, the structure and function of the actin cytoskeleton in yeast may be subject to feedback regulation by a mechanism which senses whether cell expansion is water limited.

We would like to acknowledge the assistance of Arunima Misra and Noelle Dwyer in the early phases of this work and Richard Gomer, Michael Stern, and members of the Gustin laboratory for helpful comments on the manuscript. We thank the Botstein lab for yeast strains, A. Adams for the *SAC6* clone, B. Haarer for the *PFY1* clone, A. Bretscher for the *TPM1* clone, J. Cooper for the *CAP2* clone, and T. Dunn for the *SAC7* clone.

This work was supported by the National Science Foundation (DCB8904045).

References

Adams, A. E. M., and J. R. Pringle. 1984. Relationship of actin and tubulin distribution to bud growth in wild-type and morphogenetic-mutant *Saccharomyces cerevisiae*. *J. Cell Biol.* 98:934–945.

Adams, A. E. M., and D. Botstein. 1989. Dominant suppressors of yeast actin mutation that are reciprocally suppressed. *Genetics*. 121:675–683.

Adams, A. E. M., and J. R. Pringle. 1991. Staining of actin with fluorochrome-conjugated phalloidin. *Methods Enzymol.* 194:729–731.

Adams, A. E. M., D. Drubin, and D. Botstein. 1989. A yeast actin-binding protein is encoded by *SAC6*, a gene found by suppression of an actin mutation. *Science (Wash. DC).* 243:231–233.

Adams, A. E. M., D. Botstein, and D. Drubin. 1991. Requirement of yeast fimbrin for actin organization and morphogenesis *in vivo*. *Nature (Lond.).* 354:404–408.

Amatruda, J. F., J. F. Cannon, K. Tatchell, C. Hug, and J. A. Cooper. 1990. Disruption of the actin cytoskeleton in yeast capping protein mutants. *Nature (Lond.).* 344:352–354.

Barnes, G., D. G. Drubin, and T. Stearns. 1990. The cytoskeleton of *Saccharomyces cerevisiae*. *Curr. Op. Cell. Biol.* 2:109–115.

Blomberg, A., and L. Adler. 1989. Roles of glycerol and glycerol-3-phosphate dehydrogenase (NAD^+) in acquired osmotolerance of *Sacharomyces cerevisiae*. *J. Bacteriol.* 171:1087–1092.

Brown, A. D. 1978. Compatible solutes and extreme water stress in eukaryotic microorganisms. *Adv. Microb. Physiol.* 7:181–242.

Cleves, A. E., P. J. Novick, and V. A. Bankaitis. 1989. Mutations in the *SAC1* gene suppress defects in yeast golgi and yeast actin function. *J. Cell Biol.* 109:2939–2950.

Cooper, J. A. 1987. Effects of cytochalasin and phalloidin on actin. *J. Cell Biol.* 105:1473–1478.

Cosgrove, D. 1986. Biophysical control of plant cell growth. *Ann. Rev. Plant Physiol.* 37:377–405.

Dale, J. E., and J. F. Sutcliffe. 1986. Water relations of plant cells. *In* Plant Physiology. A Treatise, Vol. IX: Water and Solutes in Plants. Academic Press, Inc., NY. 1–48.

Drubin, D. G. 1990. Actin and actin-binding proteins in yeast. *Cell Motil. Cytoskeleton.* 15:7–11.

Drubin, D. G., K. G. Miller, and D. Botstein. 1988. Yeast actin binding proteins: evidence for a role in morphogenesis. *J. Cell Biol.* 107:2551–2561.

Dunn, T. M., and D. Shortle. 1990. Null alleles of *SAC7* suppress temperature-sensitive actin mutations in *Saccharomyces cerevisiae*. *Mol. Cell. Biol.* 10:2308–2314.

Gallwitz, K., and R. Seidel. 1980. Molecular cloning of the actin gene from yeast *Saccharomyces cerevisiae*. *Nucleic Acids Res.* 8:1043–1059.

Gallwitz, K., and I. Sures. 1980. Structure of a split yeast gene: complete nucleotide sequence of the actin gene in *Saccharomyces cerevisiae*. *Proc. Natl. Acad. Sci. USA.* 77:2546–2550.

Gustin, M. C., X. L. Zhou, B. Martinac, and C. Kung. 1988. A mechanosensitive ion channel in the yeast plasma membrane. *Science (Wash. DC).* 242:762–776.

Haarer, B. K., S. H. Lillie, A. E. M. Adams, V. Magdolen, W. Bandlow, and S. S. Brown. 1990. Purification of profilin from *Saccharomyces cerevisiae* and analysis of profilin-deficient cells. *J. Cell Biol.* 110:105–114.

Hartwig, J. H., and D. J. Kwiatkowski. 1991. Actin-binding proteins. *Curr. Op. Cell Biol.* 3:87–97.

Huffaker, T. C., M. A. Hoyt, and D. Botstein. 1987. Genetic analysis of the yeast cytoskeleton. *Annu. Rev. Genet.* 21:259–284.

Johnson, G. D., and G. M. de C. Nogueira Arauja. 1981. A simple method of reducing the fading of immunofluorescence during microscopy. *J. Immunol. Meth.* 43:349–350.

Kilmartin, J. V., and A. E. M. Adams. 1984. Structural rearrangements of tubulin and actin during the cell cycle of the yeast *Saccharomyces*. *J. Cell Biol.* 98:922–933.

Liu, H., and A. Bretscher. 1989. Disruption of the single tropomyosin gene in yeast results in the disappearance of actin cables from the cytoskeleton. *Cell.* 57:233–242.

Luna, E. J. 1991. Molecular links between the cytoskeleton and membranes. *Curr. Op. Cell Biol.* 3:120–126.

Matsudaira, P. 1991. Modular organization of actin crosslinking proteins. *Trends Biochem. Sci.* 16:87–92.

Ng, R., and J. Abelson. 1980. Isolation and sequence of the gene for actin in *Saccharomyces cerevisiae*. *Proc. Natl. Acad. Sci. USA.* 77:3912–3916.

Novick, P., and D. Botstein. 1985. Phenotypic analysis of temperature-sensitive yeast actin mutants. *Cell.* 40:415–426.

Novick, P., B. C. Osmond, and D. Botstein. 1989. Suppressors of yeast actin mutations. *Genetics.* 121:659–674.

Ortega, J. K. E., E. G. Zehr, and R. G. Keanini. 1989. *In vivo* creep and stress relaxation experiments to determine the wall extensibility and yield threshold for the sporangiophores of *Phycomyces*. *Biophys. J.* 56:465–475.

Pringle, J. R., and I. H. Hartwell. 1981. The *Saccharomyces cerevisiae* cell cycle. *In* The Molecular Biology of the Yeast Saccharomyces. Life Cycle and Inheritance. J. N. Strathern and E. W. Jones, editors. Cold Spring Harbor Laboratory Press, Cold Spring Harbor, New York. 97–142.

Pringle, J. R., R. A. Preston, A. E. M. Adams, T. Sterns, D. G. Drubin, B. K. Haarer, and E. W. Jones. 1989. Fluorescence microscopy methods for yeast. *Meth. Cell Biol.* 31:357–435.

Reed, R. H., J. A. Chudek, R. Foster, G. M. Gadd. 1987. Osmotic significance of glycerol accumulation in yeasts. *Appl. Env. Microbiol.* 53:2119–2123.

Rine, J. 1991. Gene overexpression in studies of *Saccharomyces cerevisiae*. *Methods Enzymol.* 194:239–251.

Rodriguez, J. R., and B. M. Patterson. 1990. Yeast heavy chain mutant: maintenance of the cell type specific budding pattern and the normal deposition of chitin and cell wall components requires an intact myosin heavy chain gene. *Cell Motil. Cytoskeleton.* 17:301–308.

Sherman, F., G. R. Fink, and J. B. Hicks. 1983. *Methods in Yeast Genetics*. Cold Spring Harbor Laboratory Press, Cold Spring Harbor, NY.

Shortle, D., J. E. Haber, and D. Botstein. 1982. Lethal disruption of the yeast actin gene by integrative DNA transformation. *Science (Wash. DC).* 217:371–373.

Shortle, D., P. Novick, and D. Botstein. 1984. Construction and genetic characterization of temperature-sensitive alleles of the yeast actin gene. *Proc. Natl. Acad. Sci. USA.* 81:4889–4893.

Sonobe, S., and H. Shibaoka. 1989. Cortical fine actin filaments in higher plant cells visualized by rhodamine-phalloidin after pre-treatment with m-maleimidobenzoyl-N-hydroxysuccinamide ester. *Protoplasma.* 148:80–86.

Wulf, E. A., A. Deboben, F. A. Bautz, H. Faulstich, and T. Wieland. 1979. Fluorescent phallotoxin, a tool for the visualization of cellular actin. *Proc. Natl. Acad. Sci. USA.* 76:4498–4502.